Halogenated Greenhouse Gases Made Global Warming Primarily

Qing-Bin Lu (qblu@uwaterloo.ca)
University of Waterloo

Physical Sciences - Article

Keywords:

Posted Date: January 13th, 2022

DOI: https://doi.org/10.21203/rs.3.rs-1230021/v1

Halogenated Greenhouse Gases Made Global Warming Primarily

Qing-Bin Lu

Department of Physics and Astronomy and Departments of Biology and Chemistry, University of Waterloo, 200 University Avenue West, Waterloo, Ontario, Canada (Email: qblu@uwaterloo.ca)

Abstract: Time-series observations of global lower stratospheric temperature (GLST), global land surface air temperature (LSAT), global mean surface temperature (GMST), sea ice extent (SIE) and snow cover extent (SCE), together with observations reported in Paper I, combined with theoretical calculations of GLSTs and GMSTs, have provided strong evidence that ozone depletion and global climate changes are dominantly caused by human-made halogen-containing ozone-depleting substances (ODSs) and greenhouse gases (GHGs) respectively. Both GLST and SCE have become constant since the mid-1990s and GMST/LSAT has reached a peak since the mid-2000s, while regional continued warmings at the Arctic coasts (particularly Russia and Alaska) in winter and spring and at some areas of Antarctica are observed and can be well explained by a sea-ice-loss warming amplification mechanism. The calculated GMSTs by the parameter-free warming theory of halogenated GHGs show an excellent agreement with the observed GMSTs after the natural El Niño southern oscillation (ENSO) and volcanic effects are removed. These results provide a convincing mechanism of global climate change and will make profound changes in our understanding of atmospheric processes. This study also emphasizes the critical importance of continued international efforts in phasing out all anthropogenic halogenated ODSs and GHGs.

Introduction

It is generally agreed in the literature that the measured global mean surface temperature (GMST) had a clear rise of approximately 0.6 K between 1950 (more precisely 1975) and around 2000, coinciding with a rise in atmospheric CO_2 level. There were several reports of global warming stopping for the period between 2000 and around 2015[1-9], whereas the GMST appears to have risen again in recent years. It is also generally agreed that El Niño southern oscillation (ENSO) is one of the largest sources of year-to-year variability, but it is not likely the main cause. This paper is devoted to understanding global climate change since the late half of the 20th century when the emission of human-made halogenated gases (mainly, chlorofluorocarbons—CFCs) into the atmosphere became significant.

In the preceding paper (Paper I)[10], the author reported the discovery of a large, deep and all-season ozone hole over the tropics and the data showed the formation of three 'temperature holes' corresponding to the ozone holes over the Antarctic, tropical and Arctic respectively. The lower stratospheric temperatures (LSTs) in the three "holes" are fairly well reproduced by the cosmic-

ray-driven electron reaction (CRE) equation with the total concentration of anthropogenic halogenated ozone-depleting substances (ODS) (mainly CFCs) and cosmic ray (CR) intensity in the stratosphere as only two variables. This is also true for the extratropic/extrapolar regions (not shown in Paper I). This means that the global lower stratospheric temperature (GLST) has been controlled primarily by halogenated ODS (CFCs) and CRs. Despite its striking contrast to the expectation from current climate models, this conclusion is solidly supported by substantial observed datasets, as will be presented in this paper. It is generally agreed that the change in GLST should mirror the change in GMST. Indeed, a CFC-warming theory of GMST has been proposed by the author in previous publications[1,3,6,9].

After removal of the CR effect, the Antarctic ozone hole has shown a clear recovery since the mid-1990s, closely following the change trend of anthropogenic ODSs[6,9,11]. A similar conclusion was also reached by others[12]. The total ODS level has turned to a declining trend measured in the troposphere since around 1994 due to the Montreal Protocol[13]. It is reasonable to expect a similar trend for the Arctic ozone hole, though the latter was not significant for every spring Arctic. In contrast, the recovery of the tropical ozone hole or ozone at mid-latitudes in the lower stratosphere was delayed by around a decade from the declining trend of ODSs[6,9-11].

Given the observations outlined above, it is important to understand why there was a warming stopping in 2000-2015 and why the GMST has risen again in recent few years. An associate question is: which greenhouse gas (GHG) is dominantly governing global climate change, CFCs or CO_2? This paper aims to answer this question using substantial observation datasets including GLST, land surface air temperature (LSAT), sea ice extent (SIE), snow cover extent (SCE), GMST, as well as straightforward quantum-physical model calculations of GMST.

Here, we make a statement for the studies including Paper I[10] and this paper: we choose to use observed data as direct as possible when available instead of 'adjusted' or 'processed' data based on understanding in current climate models. The latter has led to changes in historical observed datasets. For example, the IPCC AR5 assessed estimate for historical warming between 1850–1900 and 1986–2005 was 0.61 [0.55 to 0.67] °C, while it has been changed to 0.69 [0.54 to 0.79] °C in AR6 for this same warming period due to 'changes in observational understanding'[14]. Similar 'adjustments' since 2013 can be found in most data sources used in the Report. This could create errors, given that current climate models have still significant discrepancies from observations.

Results and Discussion

(I) Global lower stratospheric temperatures (GLSTs). Furthering the presentation of time-series annul mean LST anomaly datasets at the lower stratospheres (100-30 hPa) over the polar regions and the tropics since the 1960s in Paper I[10], we plot the LSTs of southern hemisphere (SH) extratropic (30°S-90°S), northern hemisphere (NH) extratropic (30°N-90°N) and the global (90°S-90°N) from the same multiple data sources, as shown in Figure 1. Note again that the LST anomalies in original datasets were normalized to various reference temperatures and had therefore to be offset to compare with each other, but this offsetting has no effects on their long-term trends. Here, the original LST anomalies are offset to the same level in the 2000s-2010s, during which all the datasets were available and they should have smaller uncertainties than earlier measurements. There are large discrepancies between ground-based and satellite-based measured data prior to 1995. Interestingly, however, the LSTs from all measured datasets consistently show clear drops between the late 1970s and 1995 and have become constant since the mid-1990s with no significant change over the last two decades.

Given transport lags of 1 and 10 years for ODSs transported from the troposphere/surface to the lower stratosphere over the polar regions and the tropics respectively and an estimated lag of 5 years for mid-latitudes (30°N-60°N and 30°S-60°S), we get transport lags of approximately 4 and 7 years of ODSs respectively for the NH/SH extratropic and global mean lower stratospheres to model the LSTs using the CRE equation. To keep the simplicity, we use the same constants k_{Ant} and k_{Tro} to calculate the LSTs of the extratropic and the global as those used for calculating LSTs over the polar regions and the tropics in Paper I respectively, except using respective different transport lags of 4 and 7 years for ODSs. That is, *no optimizations to get the best fitting results are performed*. This is expected to cause some discrepancy between observed and calculated data for extratropic LSTs, but it should be a good approximation for the GLST, considering that the tropical area is nearly double the total area of the South and North polar regions and the tropical ozone/temperature hole is all-season in contrast to the seasonal polar holes. The thus calculated results of LSTs are also shown in Figure 1, which match the observed data surprisingly well, especially for GLSTs (as expected). Overall, the calculated curves show excellent agreements with observed data since 1995. It is worth noting the complexity that CFCs themselves are highly effective GHGs, which tend to cause stratospheric cooling too; the destruction of CFCs in the lower stratospheres over the polar regions and the tropics (shown in Paper I) should reduce this

cooling effect, compared with that over mid-latitudes. However, the stratospheric cooling effect of ozone depletion should be dominant. In spite of the obvious simplifications and approximations in above CRE-model calculations, both observed and calculated results clearly demonstrate that both extratropical and global LSTs have well been controlled only by the level of halogenated ODSs and the CR intensity and that stratospheric cooling has stopped since the mid-1990s with no significant change over the past 20 years. This is consistent with the measured trend in ODSs and observed recovery in ozone depletion shown in Paper I. Then, an obvious question arises: why has the GMST risen again in recent few years (after 2015)?

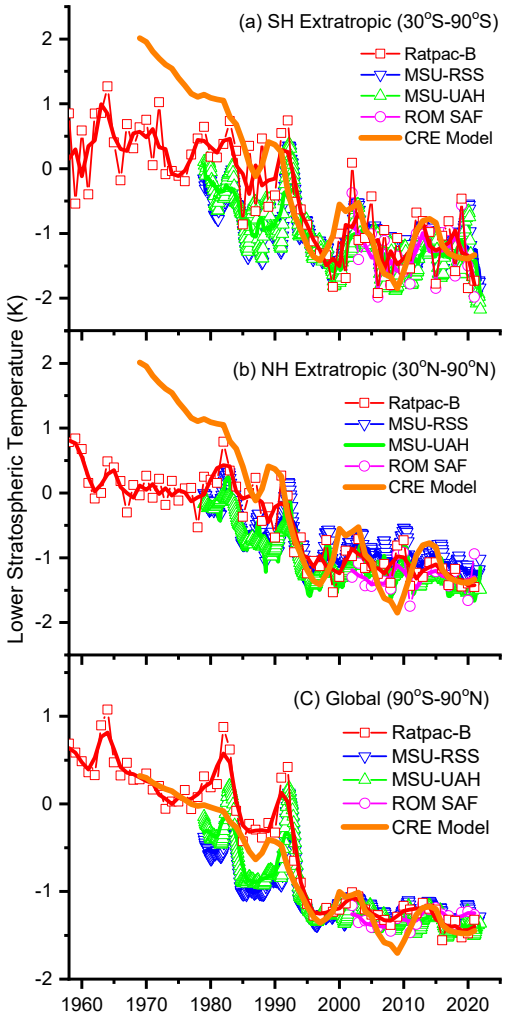

Figure 1. Time-series annul mean lower stratospheric temperature anomaly datasets of SH extratropic (30°S-90°S), NH extratropic (30°N-90°N) and the global (90°S-90°N) since 1958, obtained from multiple ground- and satellite-based data measurements (Ratpac, MSU-UAH, MSU-RSS and ROM SAF), as well as temperatures calculated by the

CRE equation (thick solid lines in orange, see text). Also shown are the 3-year smoothing (thick solid lines in colors) to observed temperature anomalies (symbols).

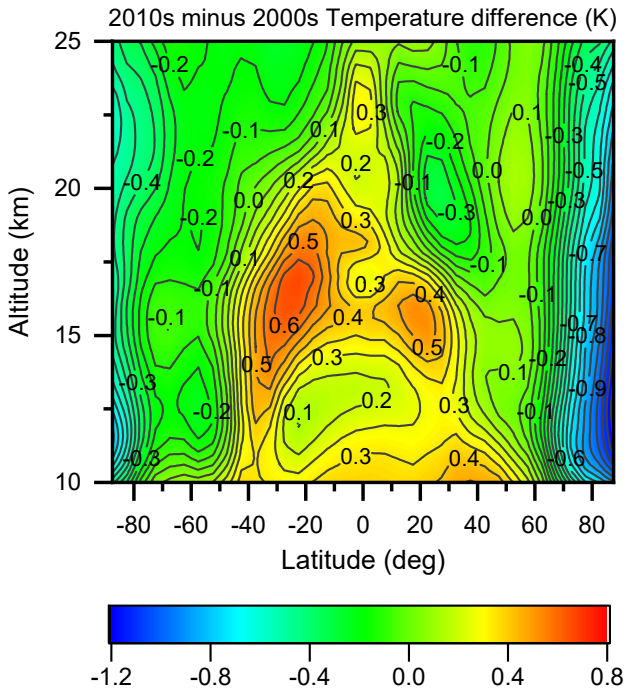

Figure 2. Difference in decadal mean zonal mean latitude-altitude distribution of the temperature climatology in the lower stratosphere at altitudes of 10-25 km of 2010-2020 minus 2000-2010.

To answer the above question, we further show the annul mean zonal mean latitude-altitude distribution of the GLST difference at altitudes of 10-25 km of the 2010s minus the 2000s, obtained from the ROM SAF satellite datasets, as plotted in Figure 2. Now, very interesting results are observed. First, stratospheric cooling in the tropics and mid-latitudes has been reversed over the past decade, which is consistent with the observed recovery of the tropical ozone hole shown in Paper I. Second, this reversal has not yet occurred over the Antarctic and even there has been a small increase in stratospheric cooling at 80°-90° S, in contrast to the observed clear recovery of the Antarctic ozone hole. Third, stratospheric cooling over the Arctic is significantly *enhanced* especially at high latitudes of 70°-90° N, in spite of no enlarging in the Arctic ozone hole. These results indicate that there is another process that is significantly affecting the regional LST at high latitudes of 70°N-90° N and 80°N-90° S.

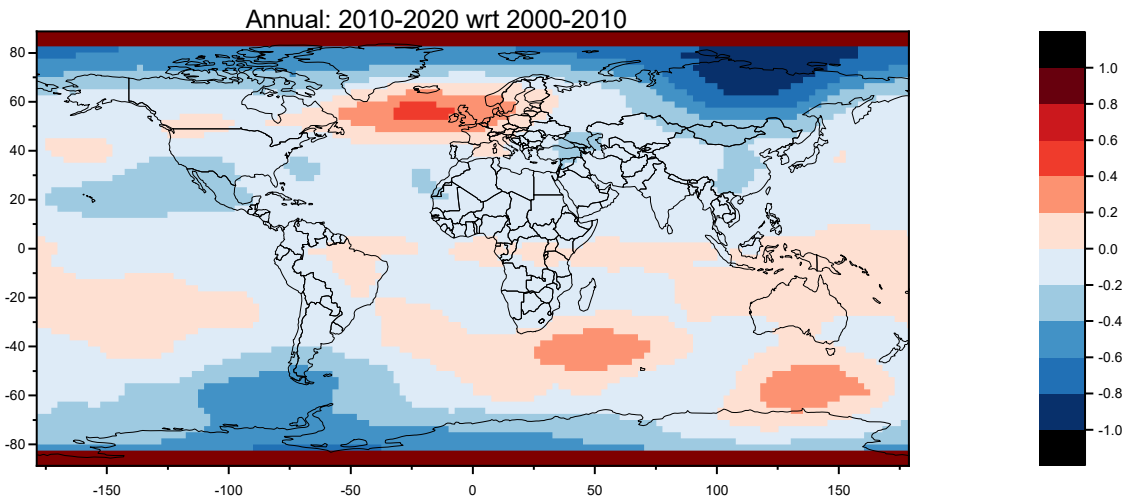

Figure 3. The map for the annul mean global lower stratospheric temperature (GLST) difference of the 2010s (2010-2020) minus the 2000s (2000-2010).

To solve the above mystery, it is important to obtain more detailed information from the map of GLST, which is made from available MSU-UAH satellite datasets[15]. The map for the annul mean GLST difference of the 2010s minus the 2000s is shown in Figure 3. It is now clearly revealed that stratospheric cooling is indeed being reversed in majority of global areas, with exceptions in some local high-latitude Arctic and Antarctic areas. The enhanced stratospheric cooling is most marked in the north and northeastern Russia, extending to the Far-East region and Alaska; it also occurs at some areas of Antarctica, especially at the region of 60°S-90°S, 50-100° W. This regional/local phenomenon cannot arise from ODSs and associated ozone depletion. It must originate from a different mechanism, which will be revealed by observed data to be presented below.

(II) Global land surface air temperatures (LSATs), sea ice extent (SIE) and snow cover extent (SCE). Since the LST change mirrors the surface temperature change, we turn to investigate the detailed changes in maps of GMST. Here we will focus more on analyzing changes in global LSAT than GMST for the following two reasons: (i) The temperature rise over land have been larger than over the oceans since 1850–1900; (ii) GMST is a combination of LSAT and sea surface temperatures (SSTs), whereas there are distinct differences between SSTs and marine air temperatures (MATs), leading to long-term trend differences between GMST and global surface air temperature (GSAT) that is the combination of LSAT and MATs by ±10% with poor theoretical understanding. Therefore, we focus on LSAT maps, which are made from the UK Met Office's

CRUTEM5 global gridded monthly (land) air temperature dataset. The maps for annual mean LSAT differences of 2000-2020 minus 1950-1975 and 2010-2020 minus 2000-2010 are shown in Figure 4 (a) and (b) respectively. Figure 4(a) clearly shows a significant and highly inhomogeneous global warming in the late half of last century. In contrast, Figure 4(b) shows that, consistent with the above observations in GLST (Figure 3), surface warming stopping or reversal has occurred in most areas of the globe and only regional warming has continued in north and northeastern coasts of Russia and in Alaska of USA since the 2000s. The continued warming over some areas at Antarctica is not visible in Figure 4(b), which is probably due to few measurement stations at Antarctica.

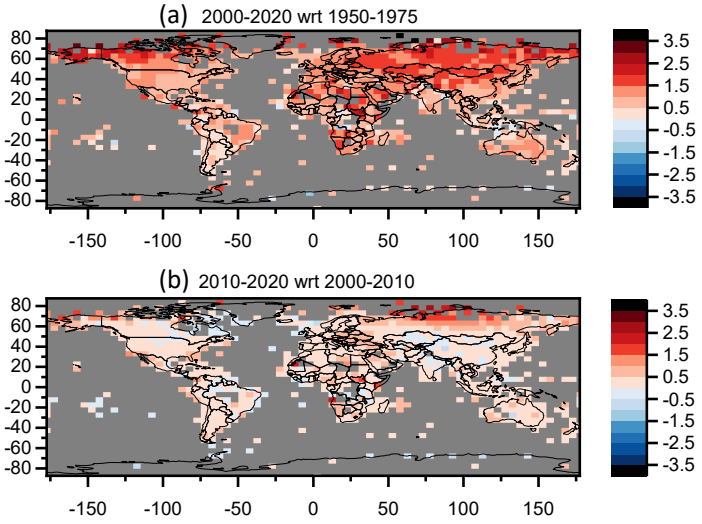

Figure 4. Maps for annul mean global land surface air temperature **(**LSAT) differences of 2000-2020 minus 1950-1975 and 2010-2020 minus 2000-2010.

To reveal the mechanism for these regional warmings, it is worth noting the cause of the so-called 'Arctic amplification (AA)' phenomenon in the observed much faster warming in the Arctic than the rest of the world over the last half century. Although the precise mechanism for AA is still under debate, there is an interesting mechanism proposed by Dai et al.[16] that AA is closely related to the surface albedo feedback associated with sea-ice loss, leading to increased outgoing longwave radiation and heat fluxes from newly opened waters. This mechanism was shown to be effective only from October to April and only over areas with significant sea-ice loss and to largely disappear when the sea ice is fixed or melts away. This AA mechanism is obviously consistent with the observed GLST results shown in Figures 2-4. Furthermore, it also agrees with the

observed seasonal NH LSAT difference of 2010-2020 minus 2000-2010 as shown in Figure 5, which shows that continued regional warming at the Arctic coasts only occurs in the seasons of DJF (December, January and February) and MAM (March, April and May) but not JJA and SON. Moreover, NH and SH sea-ice extent (SIE) data shown in Figure 6 indeed confirm the continued sea ice loss over the Arctic and the sudden melting at Antarctica around 2015. Over the past two decades, the GMST has been at its highest records since 1850 with a rise of 0.6-0.8 °C higher than that in 1950-1975. Thus, *even a small decrease in GMST will not stop ice melting at the Arctic*. By contrast, the SIE at Antarctica had a gradual *increase* from 1980 to 2015 and had an abrupt drop around 2015. This difference in SIE change between the Arctic and Antarctic can be well explained by the large O_3 loss over the Antarctic (O_3 itself is an effective GHG) in 1980-2015, which countered the warming effect caused by man-made GHGs whether CFCs or CO_2, which will be addressed below. Thus, the warming was much milder over the SH than the NH in 1980-2015. The recovery of the Antarctic O_3 hole is changing this trend. From the observed results shown in Figures 1-6, we can make a solid conclusion that regional warmings at the Arctic coasts of Russia and Alaska (USA) and some areas of Antarctica is due to continued/new sea ice loss.

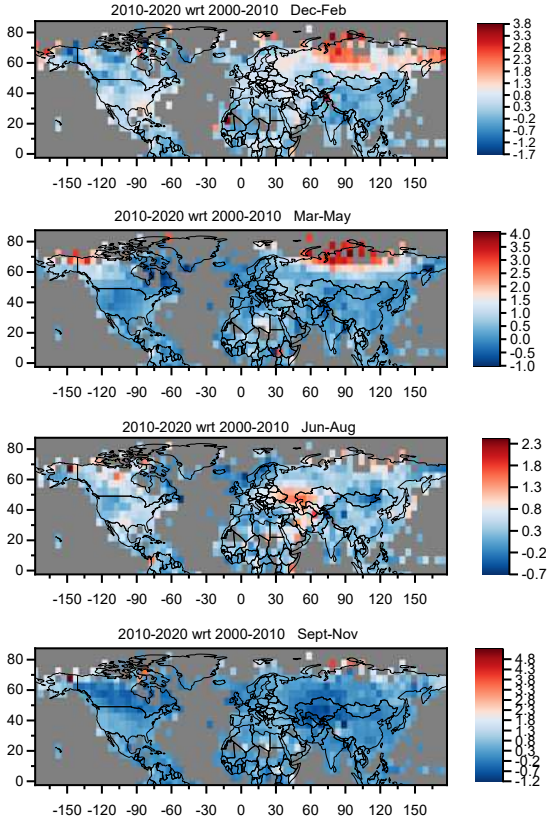

Figure 5. Maps for seasonal NH land surface air temperature (LSAT) differences of 2010-2020 minus 2000-2010.

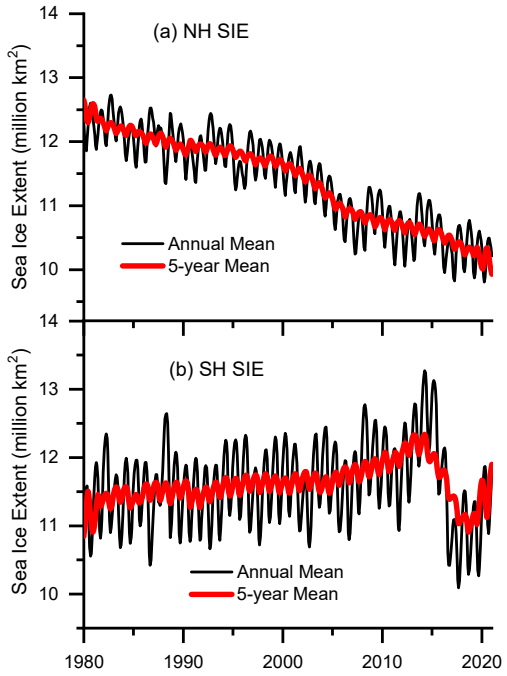

Figure 6. Time series sea ice extent (SIE) in the SH and NH during 1980-2021.

So far, all the observed data are consistent with the global warming mechanism caused by human-made halogen-containing GHGs (CFCs, HCFCs, HFCs, and PFCs). The major contribution was from CFCs up to the 2000s, while the contributions of HCFCs, HFCs and PFCs are increasing[14]. According to this mechanism, the reversal in global warming should first occur at high-latitude regions if there were no sea-ice-loss caused AA effect discussed above, as CFCs are more effectively destroyed by the CRE mechanism at high latitudes[6,9,11]. To confirm this, time-series LSAT at NH extratropic (latitudes 30°N-90° N) excluding Russia and Alaska since 1950, obtained from the UK Met Office's CRUTEM4.6 dataset, is shown in Figure 7, in which the natural El Niño and volcanic effects were removed with details given in Supplementary Information (SI) and discussed below. The result in Figure 7 indeed shows a warming stopping that is consistent with that of the total level of halogenated GHGs; the surface temperature has reached a peak at 2010-2020. Consistently, all surface temperature changes in regions or individual countries of North America (Canada, contiguous USA and Greenland), North Europe (Sweden, Norway, Finland, UK, Ireland and Iceland), and North Asia including 12 countries plus 12 north and west provinces of China show a similar warming-stopping behavior, as shown in Figure 8. Note that for these regional LSAT changes, the natural El Niño and volcanic effects were not

removed as it was hard to do so for local regions or individual countries. A similar result can be found from the UK Met Office's central England temperature (CET) dataset[17], which is the longest instrumental record of temperature in the world started in 1659, as shown in Figure S1. Moreover, time-series snow cover extent (SCE) data over NH and North America since 1965 are shown in Figure 9, both of which exhibit stabilized since ~1995. All these observed data point to a fact that global warming has stopped since around 2005.

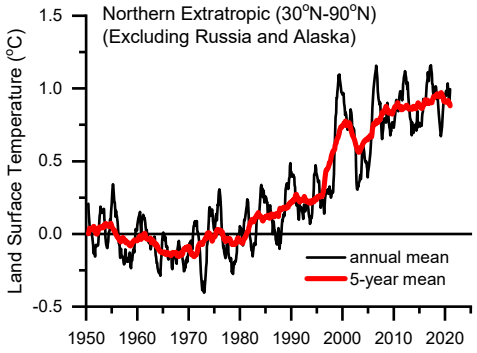

Figure 7. Time-series land surface air temperature at NH extratropic (30°N-90° N) excluding Russia and Alaska.

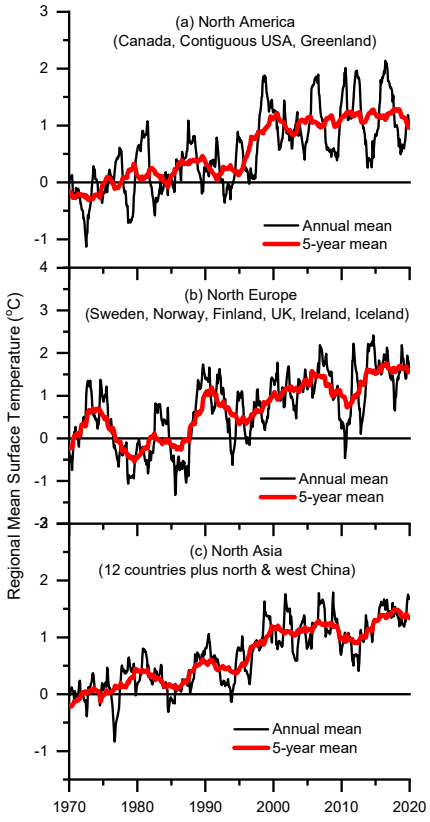

Figure 8. Time Series surface temperatures in North America (Canada, contiguous USA and Greenland), North Europe (Sweden, Norway, Finland, UK, Ireland and Iceland) and North Asia including 12 countries plus 12 north and west provinces of China.

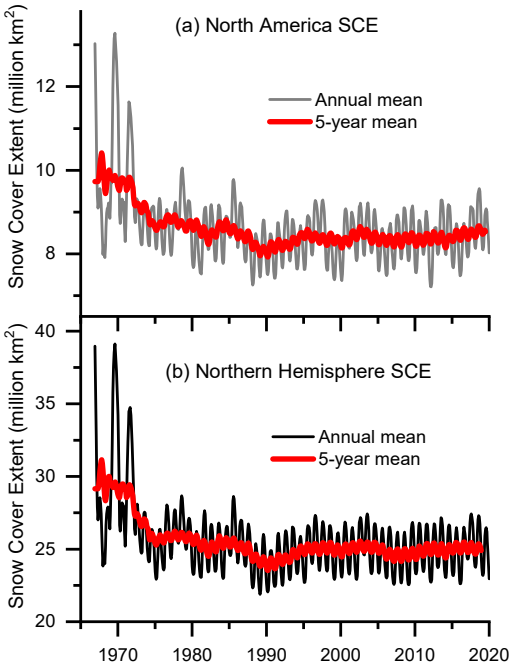

Figure 9. Time series snow cover extent (SCE) in the NH and North America during 1968-2020.

In striking contrast to the excellent agreement between observed data in Figures 1-9 and the warming mechanism of halogenated GHGs, these robust observations do not agree with current climate models which give GMST rises caused dominantly by radiative forces of increased CO_2, CH_4 and N_2O atmospheric concentrations. Note that there is no current controversy about the fact that the absorption of terrestrial radiation emitted from the earth surface by these major non-halogen GHGs at the centers of their IR bands (e.g., CO_2 at 667 cm^{-1}) has been entirely saturated. What is under the current debate is whether the absorption at the edge wings of their IR bands would continue to increase with rising gas concentrations and contribute considerably to the observed global surface temperature change. In current climate models, it is assumed that the greenhouse effect of these major GHGs is not yet saturated and non-linear (e.g., logarithmic for CO_2) relationships between the radiative force ΔF and gas concentration for CO_2, CH_4 and N_2O are applied, in contrast to a linear relationship for halogenated GHGs. As the author pointed out previously[3,6,9], there are at least two major problems with this assumption. From a fundamental radiation physics point of view, if the absorption at the edge wings of the IR bands of CO_2, CH_4 and N_2O had not been saturated, the extent of saturation in overall IR absorption by these GHGs would increase with increasing gas concentrations. This actually contradicts the observed fact.

Whether the first-generation or state-of-the-art climate models (AOGCMs) has given an identical radiative forcing $\Delta F \approx 0.72$ W.m^{-2} for the CO_2 concentration rises of 285 to 326 ppm in 1850-1970 and of 326 to 373 ppm in 1970-2002. This radiative forcing would cause a global surface temperature rise of about 0.6 °C, given the equilibrium climate sensitivity factor λ_c=0.8 K/(W/m^2), which is consistent with the observed GMST rise in 1970-2002. However, the observed GMST rise in 1850-1970 was 0.1-0.2°C, far less than 0.6 °C. From a direct observation point of view, the above assumption in standard climate models has in fact been disapproved by observed data already. The greenhouse effect of rising CO_2, CH_4 and N_2O can be detected from variations in the radiance spectrum of outgoing longwave radiation (OLR) at the top of atmosphere, which carries the signature of greenhouse gases that cause the warming effect. The difference spectrum between the spectra of the OLR of the Earth as measured by the NASA Infrared Interferometric Spectrometer (IRIS) onboard the Nimbus 4 spacecraft in 1970[18] and the interferometric monitor for greenhouse gases (IMG) onboard the ADEOS satellite in 1997[19] has provided important information on this critical issue. A preliminary study showed the consistence between observed data and climate models over the 27-year period (1970-1997) of the most rapid global warming. Particularly a negative-going brightness temperature difference was shown on the edge of the CO_2 ν_2 band, between 710 and 740 cm^{-1}, in accord with the radiative force caused by the increased CO_2 concentration. However, subsequent more robust studies of the same satellite data by Brindley and Allan[20] and Anderson *et al*.[21] independently found the striking result that the negative brightness temperature difference (by about −1.5 K) at the wing from 800 to 600 cm^{-1} of the main 667 cm^{-1} CO_2 band, expected from climate models, was absent in the observed difference spectrum. This observation is certainly of critical importance because the assumed radiative forcing (of CO_2) lies at the heart of the debate on the cause of global warming observed in the late half of the 20th century. Unfortunately these major problems with the assumption of no saturation in greenhouse effect of CO_2, CH_4 and N_2O have been ignored in current climate models. More evidence on this critical issue can be found in the author's previous publications[3,6,9].

(III) Parameter-free theoretical calculations of GMST. To compare our theoretical results with observed GMST data, it is necessary to remove the natural El Niño and volcanic effects from observed GMST data. In fact, there has been no significant volcanic effect since 2000, while El Niño southern oscillation (ENSO) is the largest source of year-to-year variability. We simply adopt

the empirical model developed by Lean and Rind[22,23], which played an important role in proving that the warming in the late half of last century was due to anthropogenic influences. In this model, lags are 4 months for ENSO, 6 months for volcanic aerosols, and 120 months for anthropogenic force. The latter (the 10-year lag), which was chosen to maximize the explained variance in Lean-Rind model, turns out to agree excellently with our observed ozone recovery trend at tropical and mid-latitudes delayed from the tropospheric halogenated ODS peak[1,6,9]. The natural contributions to the GMSTs were 0.2° C warming during major ENSO events in 1997–98, and about 0.3° C cooling in 1992 following the large Pinatubo volcanic eruption[22,23]. These values are used to remove ENSO and volcanic effects from observed GMST data without further optimization, with details given in SI and Figure S2.

In view of observations reported previously by the author[1,3,6,9], others[2,4,5,7,8,20,21], and shown in Figures 1-9 above, no warming effects of increased CO_2, CH_4 and N_2O are included in the warming model of halogenated GHGs (mainly CFCs), whose details have been given previously[9]. Note that in drastic contrast to standard climate models, *no parameter is used in the CFC-warming model*, in which equilibrium climate sensitivity (λ_c^{halo}) was determined by the product of the climate sensitivity factor (α) of halogenated GHGs in the atmospheric window at wavelengths of 8-13 μm and the feedback amplification factor (β)[9]. Both α and β were respectively obtained from quantum-physics understanding of the satellite-measured atmospheric transmittance spectrum in the atmospheric window, at which halogenated GHGs have strong infrared absorption bands, and observed surface temperature variations during solar cycles. With the determined λ_c^{halo} ($=\alpha\beta$), known radiative efficiencies and a lag of 10 years of halogenated GHGs, the physical model calculations with sole inputs of atmospheric concentrations of halogenated GHGs produce time-series GMST values. Given updated concentrations of halogenated GHGs obtained from the new IPCC AR6[14], our calculated GMST values exhibit an excellent agreement with observed GMST data since 1950s, as shown in Figure 10. Interestingly, the calculated results also match nearly perfectly the observed GMST data over the past 5 years if the regions of Russia and Alaska are excluded. These observed and theoretical results strongly indicated that climate changes in both global stratosphere and global surface have been primarily controlled by atmospheric halogenated ODSs and GHGs with interesting and complex phenomena caused by associated stratospheric ozone depletion and polar sea ice loss.

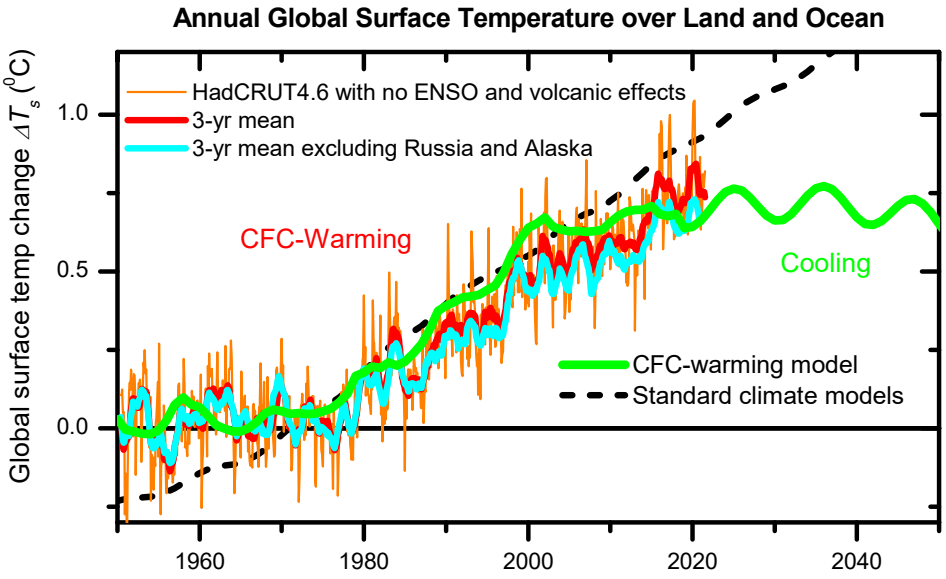

Figure 10. Observed and theoretical GMSTs. Observed GMST data were from the UK Met Office's combined land-surface air temperature and sea-surface temperature anomalies (HatCRUT4.6); the curves in red and cyan are respectively 3-point averages of observed data with and without the inclusion of Russia and Alaska. The theoretical GMSTs (the curve in green) were calculated by the CFC-warming model, including the contribution of all halogenated GHGs and the 11-year cyclic variation of ±0.05 °C due to solar cycles (see text).

Conclusions

Substantial time-series observations of global lower stratospheric temperature, global surface air temperature, sea ice extent and snow cover extent, together with observed data of stratospheric ozone depletion and stratospheric cooling reported in Paper I, combined with our theoretical calculations of lower stratospheric temperatures and global mean surface temperatures, have provided solid and convincing evidence that ozone depletion and global climate changes are dominantly caused by man-made halogen-containing ODSs and GHGs respectively. It has no doubts that CO_2, N_2O and CH_4 are important GHGs to lead to Earth's current ecological environment. However, the observed data do not indicate any signs of the greenhouse effect of *increased* concentrations of these major non-halogen GHGs since 1950. Their role in causing the GMST rise during 1950-2000 should be very minor if not zero. This conclusion is in striking contrast to that of standard climate models, but is strongly supported and consistent with solid observations presented in this study and previously[1,3,6,8,9,20,21].

Since GMST is still around the peak, ice melting at the Arctic is most likely to continue and at Antarctica may be increasing with the recovery of the Antarctic ozone hole due to the increased

greenhouse effect of recovering ozone. With the controls in production and use of CFCs, HCFCs, HFCs and PFCs by international Agreements including the highly successfully and extremely important Montreal Protocol and its Amendments, however, it is most likely to see a gradual global reversal in GMST in coming decades. Nevertheless, this reversal will come true only with continued international efforts in phasing out all halogenated ODSs and GHGs. Therefore, the tremendous efforts from international governments and community are required if humans desire to reverse the climate change caused by anthropogenic halogenated ODSs and GHGs.

ACKNOWLEDGEMENTS

The author is greatly indebted to the Science Teams for making the data used for this study available. This work is supported by the Canadian Institutes of Health Research and Natural Science and Engineering Research Council of Canada.

AUTHOR DECLARATIONS

The author has no conflicts to disclose.

DATA Sources: The data used for this study were obtained from the following sources: NOAA's Microwave Sounding Units (MSU) UAH and RSS datasets and Ratpac-B time-series dataset were obtained from NOAA; radio occultation (RO) satellite datasets were obtained from the ROM SAF; GLSAT and GMST datasets were obtained from the UK Met Office (CRUTEM4.6, CRUTEM5.0 and HadCRUT4.6); LSATs of regions or individual countries were obtained from Berkeley Earth, UK Met Office (HadCET) and NOAA (ClimDiv CONUS); sea ice extent, snow cover extent and ENSO datasets were obtained from NOAA; cosmic ray data were obtained from ref. 11; concentrations of halogenated GHGs were obtained from the 2021 IPCC AR6 Report.

References:

1 Lu, Q.-B. Cosmic-ray-driven electron-induced reactions of halogenated molecules adsorbed on ice surfaces: Implications for atmospheric ozone depletion and global climate change. Physics Reports 487, 141-167, doi:10.1016/j.physrep.2009.12.002 (2010).
2 Knight, J. et al. Do global temperature trends over the last decade falsify climate predictions. Bulletin of the American Meteorological Society 90, 22-23 (2009).
3 Lu, Q.-B. What is the major culprit for global warming: CFCs or CO_2? Journal of Cosmology 8, 1846-1862 (2010).

4 Easterling, D. R. & Wehner, M. F. Is the climate warming or cooling? Geophys. Res. Lett. 36, doi:10.1029/2009GL037810 (2009).
5 Kerr, R. A. Climate change. What happened to global warming? Scientists say just wait a bit. Science 326, 28-29, doi:10.1126/science.326_28a (2009).
6 Lu, Q.-B. Cosmic-ray-driven reaction and greenhouse effect of halogenated molecules: culprits for atmospheric ozone depletion and global climate change. Intl. J. Modern Phys. B 27, doi:10.1142/s0217979213500732 (2013).
7 Fyfe, J. C., Gillett, N. P. & Zwiers, F. W. Overestimated global warming over the past 20 years. Nature Climate Change 3, 767-769, doi:10.1038/nclimate1972 (2013).
8 Happer, W. Why has global warming paused? Intl. J. Modern Phys. A 29, 1460003, doi:10.1142/s0217751x14600033 (2014).
9 Lu, Q.-B. New Theories and Predictions on the Ozone Hole and Climate Change (*World Scientific*, 2015) pp.1-285.
10 Lu, Q.-B. Discovery of a New Ozone Hole over the Tropics, Nature, Submitted.
11 Lu, Q.-B. Fingerprints of the cosmic ray driven mechanism of the ozone hole. AIP Advances 11, 115307, doi:10.1063/5.0047661 (2021).
12 Banerjee, A., Fyfe, J., Polvani, L., Waugh, D. & Chang, K. A pause in Southern Hemisphere circulation trends due to the Montreal Protocol. Nature 579, 544-548, doi:10.1038/s41586-020-2120-4 (2020).
13 WMO/UNEP Global Ozone Research and Monitoring Project—Report No. 58. Scientific Assessment of Ozone Depletion: 2018.
14 The 2021 IPCC AR6 Report, in press.
15 Christy, J. R., Spencer, R. W. & Braswell, W. D. MSU Tropospheric Temperatures: Dataset Construction and Radiosonde Comparisons. *J. Atmos. Oceanic Technology* **17**, 1153-1170, doi:10.1175/1520-0426 (2000).
16 Dai, A., Luo, D., Song, M. & Liu, J. Arctic amplification is caused by sea-ice loss under increasing CO_2. Nature Communications 10, 121, doi:10.1038/s41467-018-07954-9 (2019).
17 Parker, D. E., Legg, T. P. & Folland, C. K. A new daily central England temperature series, 1772–1991. Intl. J. Climatology 12, 317-342, doi:10.1002/joc.3370120402 (1992).
18 Hanel, R. A. et al. The Nimbus 4 infrared spectroscopy experiment: 1. Calibrated thermal emission spectra. J. Geophys. Res. (1896-1977) 77, 2629-2641, doi:10.1029/JC077i015p02629 (1972).
19 Kobayashi, H. et al. Development and evaluation of the interferometric monitor for greenhouse gases: a high-throughput Fourier-transform infrared radiometer for nadir Earth observation. Appl. Opt. 38, 6801-6807, doi:10.1364/AO.38.006801 (1999).
20 Brindley, H. E. & Allan, R. P. Simulations of the effects of interannual and decadal variability on the clear-sky outgoing long-wave radiation spectrum. Q. J. R. Meteorol. Soc. 129, 2971-2988, doi:10.1256/qj.02.216 (2003).
21 Anderson, J. G., Dykema, J. A., Goody, R. M., Hu, H. & Kirk-Davidoff, D. B. Absolute, spectrally-resolved, thermal radiance: a benchmark for climate monitoring from space. J. Quant. Spectrosc. Radiat. 85, 367-383, doi:101016/S0022-4073(03)00232-2 (2004).
22 Lean, J. L. & Rind, D. H. How natural and anthropogenic influences alter global and regional surface temperatures: 1889 to 2006. Geophys. Res. Lett. 35, doi:10.1029/2008GL034864 (2008).
23 Lean, J. L. & Rind, D. H. How will Earth's surface temperature change in future decades? Geophys. Res. Lett. 36, doi:10.1029/2009GL038932 (2009).

Supplementary Files

This is a list of supplementary files associated with this preprint. Click to download.

- SupplementaryInformationforPaperII.pdf